Geophysical Journal (1988) **95**, 111–121

Statistical modelling of lower-crustal reflections

B. A. Raynaud*
BIRPS, Bullard Laboratory, Madingley Rise, Madingley Road, Cambridge CB3 0EZ, *UK*

Accepted 1988 April 10. Received 1988 March 29; in original form 1988 January 4

SUMMARY

For a geological feature to be resolved in a seismic reflection profile its size must be comparable with the dimensions of the Fresnel zone for its depth and the frequency-content of the seismic wavefield. Since the diameter of the Fresnel zone is over 5 km for lower-crustal reflections, the effects of variations of the crust on smaller length scales must be considered when interpreting deep reflection profiles.

Modelling the seismic wavefield using first-order scattering theory shows how the reflections observed in a small-offset profile are affected by the statistical distribution of elastic variations within the crust. Crustal heterogeneities on length-scales smaller than the seismic wavelength cause frequency-dependent attenuation which can be comparable with the losses due to anelastic absorption. Larger scale elastic variations cause rapid loss of coherence in the seismic field. The observation of deep seismic reflections can thus be used to constrain the degree to which the crustal elasticity varies on small length scales. Coherent seismic reflections from the lower crust limit the fractional variation of elasticity averaged over the entire crust to a few percent on a wide range of length-scales.

Key words: deep seismic reflection, lower-crustal reflection, statistical crustal model, first-order scattering, Born scattering

INTRODUCTION

An observed seismic reflection is made up of a superposition of components that have travelled along a range of paths within the crust (Hagedoorn 1954). The finite crustal volume sampled by a reflection limits the lateral resolution of a seismic reflection profile to the order of the Fresnel zone radius, r_F. Since r_F is over 2.5 km for near-normal-incidence reflections from the lower crust, the effects of crustal variations which are too small to be independently resolved must be considered when interpreting the structure of the lower crust from deep reflection profiles. A distribution of small-scale variations of crustal elasticity can affect an observed reflection if, in total, the variations affect a large proportion of the wavefield components that are transmitted through the sampled volume.

Provided the fractional variations of the elastic medium are small, the effects on elastic waves of small-scale variations of the medium can be modelled by perturbation theory. Either first-order (Born) scattering or multiple-scattering theories may be appropriate depending on the severity of the scattering effects.

The main formula of the first-order theory, giving the expectation of the scattered field intensity as a function of direction, was first derived by Pekeris (1947). Chernov (1960) used first-order scattering to derive a number of statistical properties of the acoustic field in a heterogeneous medium including the attenuation and loss of coherence caused by scattering. Knopoff & Hudson (1964, 1967) applied first-order theory to the elastic case showing that the acoustic approximation is valid at high frequencies, but that the degree of scattering is underestimated at low frequencies due to the neglect of P–S conversions.

First-order scattering has been used to interpret a variety of seismic experiments. It has been applied to the attenuation of the high-frequency components of teleseismic events (e.g. Aki & Chouet 1975; Aki 1981) and to estimate the variations of the earth's crust immediately below Large Seismic Arrays (e.g. Aki 1973; Capon 1974). It has also been applied to the study of the core–mantle boundary (Haddon & Cleary 1974) and used as the basis of a method for processing deep reflection sections (Phinney & Jurdy 1979).

This paper considers the effects on deep reflection profiles of small-scale variations of crustal elasticity by applying first-order scattering theory to statistical crustal models. First-order scattering is described briefly in the next section [a full derivation is given in chapter 13 of Aki & Richards (1980)] and is then applied to constrain the range of elastic impedance variations within the crust. The theory is illustrated by examples generated by a computer program which calculates the scattered field for statistically defined crustal models.

* Now at: Carrington Computer Consultants, 57a Hatton Garden, London EC1N 8JD, UK.

ELASTIC WAVES IN MILDLY HETEROGENEOUS MEDIA

A mildly heterogeneous medium can be described by writing the elastic constants in terms of mean values, ρ^0, λ^0 and μ^0, which are for simplicity assumed independent of position, and small spatially varying perturbations, ρ^1, λ^1 and μ^1

$$\rho = \rho^0 + \rho^1$$
$$\lambda = \lambda^0 + \lambda^1$$
$$\mu = \mu^0 + \mu^1.$$

To apply perturbation theory, the wavefield, $u(\mathbf{x}, t)$, is considered as the superposition of two components: a 'primary' field, $u^0(\mathbf{x}, t)$, which is the field for the unperturbed medium, and a 'scattered' field, $u^1(\mathbf{x}, t)$, which is due to the perturbations of the medium. Aki & Richards (1980) show that the scattered field at s due to an inhomogeneous crustal volume, V, centred on O is given to a first-order, linear-phase approximation by

$$\varphi(\mathbf{x}, t) = \frac{A \exp -i(\omega t - kx)}{2\Pi x} \times \int \left(ik \frac{\partial \varepsilon}{\partial \chi_i} + k^2 \varepsilon \right) \exp -i[(\mathbf{k}_{IN} - \mathbf{k}_{SC}) \cdot \boldsymbol{\chi}] \, dV_x,$$

in which x is the distance OS, A, ω and k are the amplitude, angular frequency and wavenumber of the incident wavefield, $\mathbf{k}_{IN}$ and $\mathbf{k}_{SC}$ are the wavevectors of the incident and scattered field respectively, χ_i is the component of $\boldsymbol{\chi}$ parallel to the direction of incidence and $\varepsilon(\boldsymbol{\chi})$ is the fractional variation of the elasticity at a point Q in V (Fig. 1).

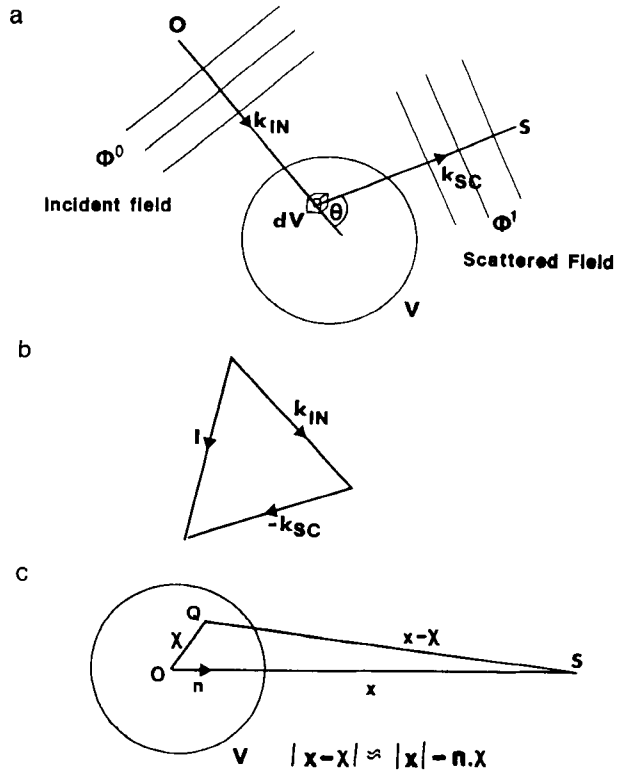

Figure 1. (a) The geometry for deriving first-order scattering theory (see text for details). (b) The definition of the scattering vector, **l**, (c) The linear phase approximation for scattered components.

Defining **l** as the scattering vector and σ as the Fourier transform of the fractional perturbation, $\varepsilon(\mathbf{x})$

$$\mathbf{l} = \mathbf{k}_{IN} - \mathbf{k}_{SC} \tag{1}$$

and

$$\sigma(\mathbf{l}) = \int \varepsilon(\boldsymbol{\chi}) \exp(-i\mathbf{l} \cdot \boldsymbol{\chi}) \, dV_x$$

$$\varepsilon(\boldsymbol{\chi}) = \frac{1}{(2\Pi)^3} \int \varepsilon(\mathbf{l}) \exp(i\mathbf{l} \cdot \boldsymbol{\chi}) \, dV_l$$

gives the amplitude of the plane component of the scattered field at S with wavevector $\mathbf{k}_{SC}$ in the form

$$\varphi_{k_{SC}}(\mathbf{x}) = \frac{Ak^2 \cos\theta}{2\Pi x} \sigma(\mathbf{l}), \tag{2}$$

in which θ is the angle between $\mathbf{k}_{IN}$ and $\mathbf{k}_{SC}$.

The intensity of the scattered field at S, $I(\mathbf{x})$, is obtained from (2)

$$I(\mathbf{x}) = \varphi(\mathbf{x})\varphi^*(\mathbf{x}) = \frac{A^2 k^4 \cos^2\theta}{(2\Pi)^2 x^2} \Sigma(\mathbf{l}), \tag{3}$$

in which $\Sigma(\mathbf{l})$ is the Fourier transform of $E(\mathbf{x})$, the autocorrelation function of the crustal variations

$$E(\mathbf{x}) = \langle \varepsilon(\boldsymbol{\chi}) \varepsilon^*(\boldsymbol{\chi} + x) \rangle \tag{4}$$

(the angled brackets represent an average over V).

The key factor in the expressions for the amplitude and intensity of the scattered field is $\sigma(\mathbf{l})$, the component of the Fourier transform of the elastic perturbations with wavevector equal to the scattering vector, **l**. Fig. 2 shows that the scattering vector for backscattering is approximately parallel to the incident wavevector with twice the magnitude. Thus backscattering is caused by variations of the medium close to the direction of incidence with a length-scale of $\lambda/2$ where λ is the wavelength of the incident wavefield.

Since the magnitude of the scattering vector cannot be greater than twice that of the incident wavevector, the wavefield only 'sees' variations of the structure with a wavelength comparable with $\lambda/2$ or greater. Variations on

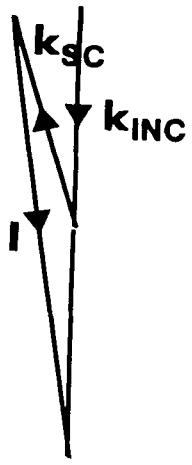

Figure 2. The scattering vector for large-angle scattering has approximately twice the magnitude of the incident wavevector and is approximately parallel to it.

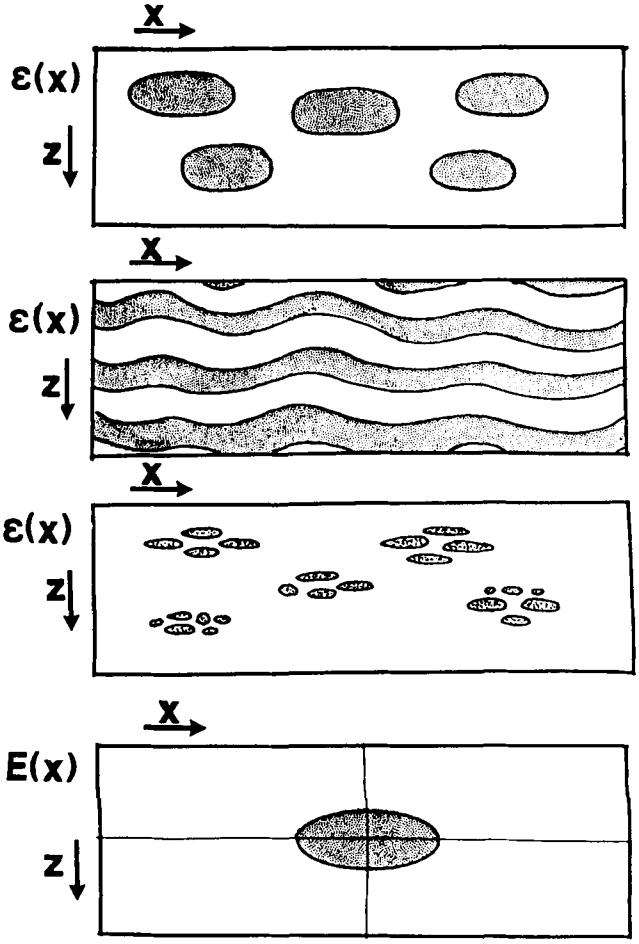

Figure 3. A variety of distributions of elastic variations, $e(\mathbf{x})$, can have similar autocorrelation functions, $E(\mathbf{x})$.

wavelengths much greater than λ cause small-angle scattering.

Very different distributions of structural variations can have similar forms of $E(\mathbf{x})$ (Fig. 3). The intensities of the scattered components produced by different distributions with the same $E(\mathbf{x})$ are indistinguishable.

COMPUTATION OF THE SCATTERED FIELD

A computer program has been written to calculate the field scattered by an arbitrary 2-D perturbation distribution according to (3). The medium is defined for the calculation by a description of the elastic properties of a 4 km square of material which represents a typical (x, z) cross-section of the crust between an upper and lower depth limit. This consists of a grid of impedance values every 40 m in the vertical direction and every 100 m in the horizontal direction. The structures at opposite sides of the structure must match because calculating the finite Fourier transform for (3) effectively assumes that the structure is repeated on a square grid.

The correlation length of the crustal structure parallel to the y-axis is assumed to be very large. It is shown below that many results of first-order scattering theory are independent of the horizontal length-scale of the heterogeneity provided that it is greater than the seismic wavelength.

The 2-D discrete Fourier transform of this structure is calculated and the components of the Fourier transformed autocorrelation function, $\Sigma(\mathbf{l})$, are found. The intensity of any scattered component can be estimated from these components according to (3). Values of $\Sigma(\mathbf{l})$ lying between the discrete values of the Fourier transform are estimated by linear interpolation since it is assumed that the magnitudes of the Fourier components vary smoothly for random structures. The scattered field for an extended heterogeneous volume is estimated by dividing the extended volume into smaller parts and superposing the fields scattered by each of these.

Figure 4 shows (x, z) cross-sections of three heterogeneous structures and the intensities of the scattered field components scattered by them through angles greater than 90° for a vertically incident field. The vertical correlation length of these structures is approximately 200 m and the impedance values of the shaded and unshaded regions differ by 10 per cent. The field components scattered by the coherent layering in Fig. 4(a) are the most concentrated in the vertical direction. The scattered components in Fig. 4(b and c) have a similar degree of vertical concentration showing that a distribution of intrusions can produce a scattered field with a degree of coherence comparable to that scattered by deformed continuous layering.

ATTENUATION DUE TO SCATTERING

From conservation of energy, the production of a scattered field must be accompanied by a reduction of the flux of the primary field. This process represents a form of attenuation of the seismic field which acts in addition to anelastic absorption to give the observed attenuation (Wu 1982, 1985).

Aki & Richards (1980) find the attenuation due to scattering by summing the flux of the scattered field produced in all directions by a cube of heterogeneous crust of side L. However, since components scattered through small angles remain mixed with the transmitted field they should not be included in the calculation of flux loss (Sato 1982a, b).

To estimate the attenuation produced by scattering in a heterogeneous crust requires a description of the distribution of elastic variations. As the lower crust is likely to have different correlation lengths in the horizontal and vertical directions (Meissner 1973), the following autocorrelation function is used to represent a structure characterized by an anisotropic distribution of perturbations with correlation lengths a and c, in the horizontal and vertical directions respectively.

$$E(\mathbf{x}) = H^2 \exp\left(-\frac{x^2+y^2}{a^2} - \frac{z^2}{c^2}\right) \tag{5}$$

$$\Rightarrow \Sigma(\mathbf{l}) = \Pi^{3/2} a^2 c H^2 \exp\left(-\frac{a^2(l_x^2+l_y^2)+c^2 l_z^2}{4}\right). \tag{6}$$

It is useful to assume that $ak \gg 1$, i.e. the horizontal correlation length of the structure is greater than the seismic wavelength. This implies that for a vertically-incident

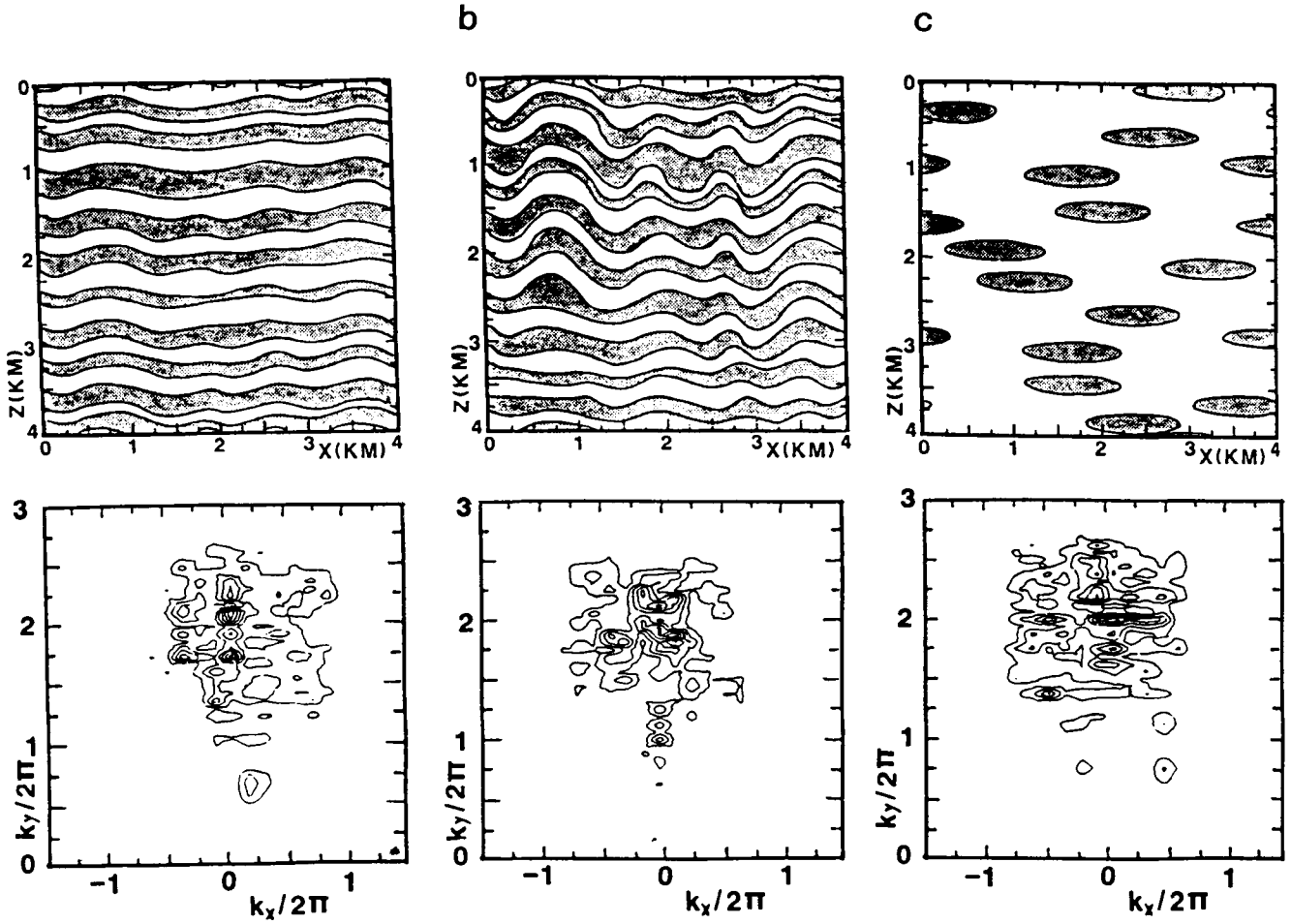

Figure 4. The scattered components produced when a vertically incident plane-wave travels for 1 km through three different distributions of crustal elasticity variations.

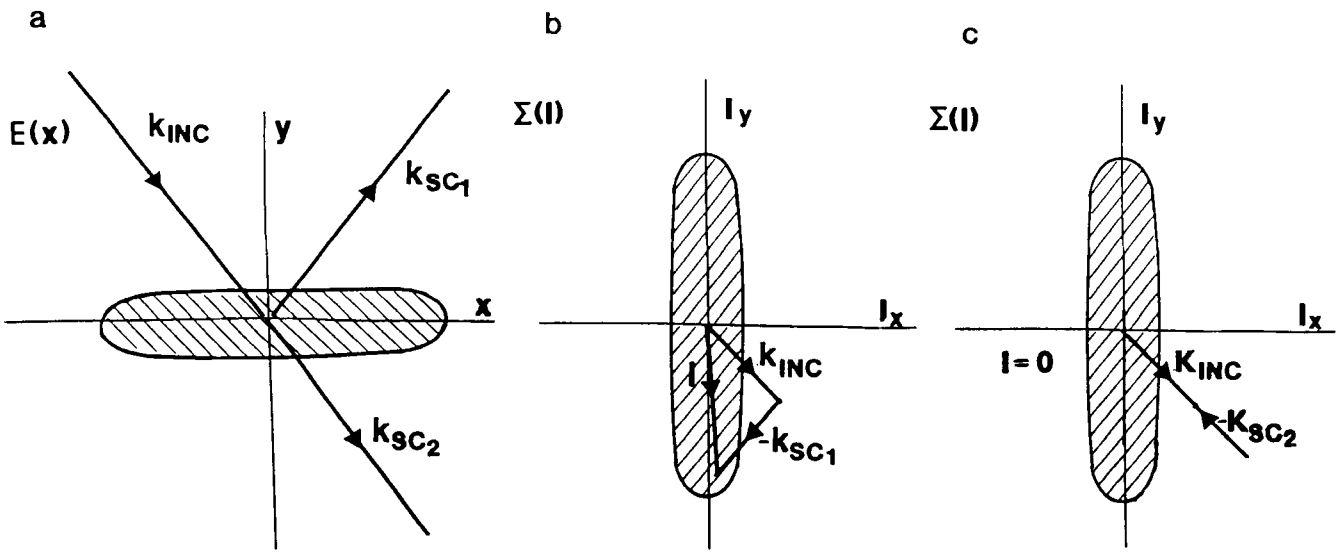

Figure 5. A set of perturbations with $ak \gg 1$ produces scattered components in two small angular ranges due to the concentration of $\Sigma(\mathbf{l})$ close to the vertical axis. (b) A set of components scattered in directions close to the wavevector for specular reflection. (c) A second set of components which is scattered through small angles and propagates in directions close to the incident wavevector with altered phase.

wavefield $\Sigma(\mathbf{l})$ is small except for θ close to 0 and Π and the scattered field is concentrated into small angular ranges around two directions representing small-angle scattering and backscattering (Fig. 5). Considering only the backscattered components gives a conservative estimate of the attenuation caused by scattering.

Substituting (6) into (3) and integrating over all directions with $\theta > 90°$ shows that if $ak \gg 1$ the total flux of the scattered field is almost independent of the lateral correlation length. The proportion of energy backscattered by a cube of heterogeneous crust of side L is given by

$$\beta_{BK} \simeq \Pi^{1/2} ck^2 H^2 L \exp(-k^2 c^2). \quad (7)$$

For the Gaussian distribution of variations used to calculate (7) the backscattered flux is peaked for values of $c = \lambda/(2^{3/2}\Pi) \simeq \lambda/9$ because the longest wavelength perturbations cause scattering through small angles and the shortest wavelength perturbations are not seen by the seismic field.

If propagation through a distance L causes a small fractional attenuation of β_{BK} due to scattering the frequency-dependent Q^{-1} value for this mode of attenuation can be approximated by

$$Q^{-1}_{SCATT} \simeq \beta_{BK}/kL.$$

Since modes of flux loss are additive the effective crustal Q including both anelastic absorption and scattering is given by

$$Q^{-1}_{TOT} \simeq Q^{-1}_{ANEL} + \Pi^{1/2} kcH^2 \exp(-k^2 c^2). \quad (8)$$

It is difficult to obtain an accurate estimate of Q for the crystalline crust and to determine any variation of Q with frequency because most methods for measuring Q give poor results when measuring low degrees of attenuation in noisy data (Meissner 1986). The observation of normal-incidence reflections from the lower crust indicates a relatively low degree of attenuation and Clowes & Kanasewich (1972) estimate that Q for the crystalline crust is in the range of 300–2000.

Figure 6 shows the variation of Q^{-1}_{TOT} as a function of c/λ for media with $H = 5$ per cent and various values of anelastic attenuation. For a range of frequencies the attenuation due to scattering alone is comparable to the mid-range of Clowes and Kanasewich's estimate of crustal attenuation. With an anelastic Q of 2000 the scattering for a crust with $H = 5$ per cent produces a Q that is less than 1000 for c values in the range $\lambda/60$ to $\lambda/4$.

Figure 7 shows the variance, H^2, of a crust consisting of two components differing in their elastic impedances by a fraction h. The greatest variance, $h^2/4$, is given by equal proportions of the two components. Fig. 6 thus shows that a crustal Q of 1000 implies that the crust cannot consist of a mixture of two components in approximately equal proportions that differ in their elastic properties by more than 10 per cent if the components are on length-scales between $\lambda/30$ and $\lambda/5$. In particular, this constrains the impedance contrast of the highly reflective laminated structures that have been proposed for the lower crust (Meissner 1986). The high reflectivity and significant

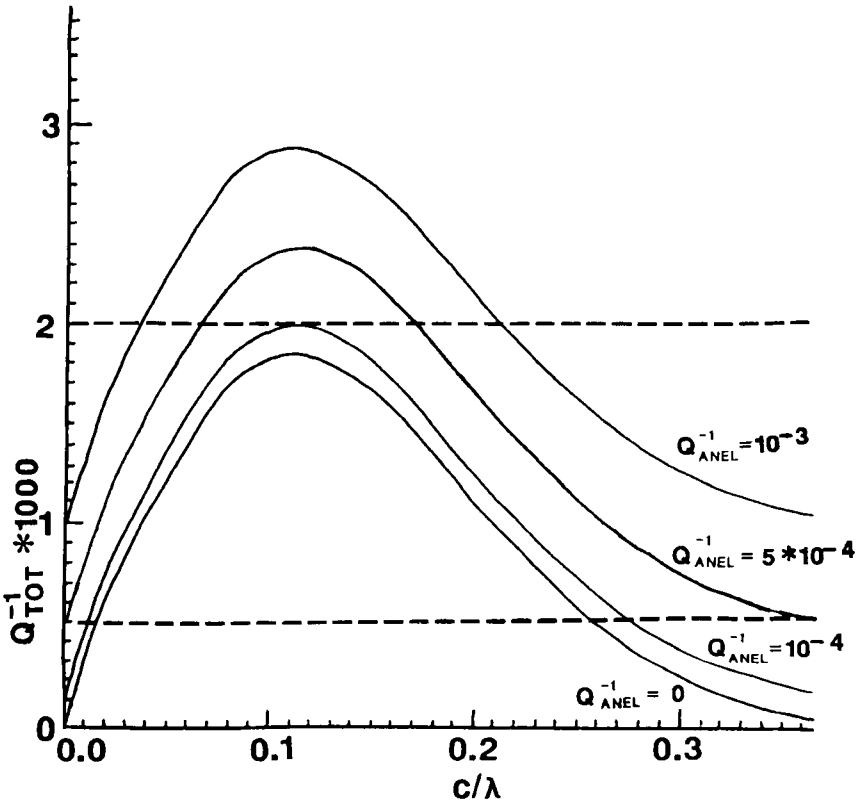

Figure 6. The variation with frequency of Q^{-1}_{TOT} due to scattering attenuation and anelastic absorption from (8). The curves correspond to anelastic absorption modelled by Q_{ANEL} values of 1000, 2000, 10 000 and ∞ (i.e. no anelastic absorption). The indicated Q values are 500 and 2000.

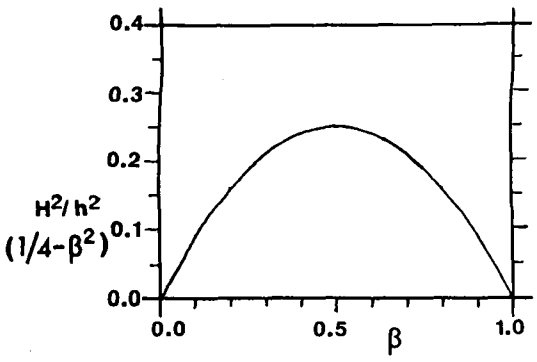

Figure 7. The variation of H^2, the variance of the elasticity of a two-phase crust, on β, the proportion of phase A. The fractional difference of the elasticity of phases A and B is h.

attenuation due to scattering of these structures are different descriptions of the same phenomena.

The frequency-dependent attenuation due to scattering can be computed for a specified heterogeneous structure by summing the scattered components. The frequency variation of Q for the three structures shown in Fig. 8 shows that higher-frequency components are generally more severely scattered, but that superimposed on this variation the attenuation is peaked for the frequency at which the vertical length scale of the perturbations is of the order of $\lambda/6$ where λ is the seismic wavelength. It should be noted that by analogy to the Gaussian distribution defined in (5) the correlation lengths of these structures are the distances at which the correlation of the variations drops to around 40 per cent is its maximum value. This length scale is smaller than the apparent length scales of the structures by a factor of around 3.5.

Figure 9 shows the attenuation for the layered structures shown in Fig. 4. Both structures show a high degree of attenuation due to scattering at around 10 Hz: the tuning of this notch is more accentuated in Fig. 9(a) which represents less deformed layering. Fig. 9(b) shows a greater degree of flux loss due to small-angle scattering.

INCOHERENCE CAUSED BY SCATTERING

The components of the wavefield scattered through small angles remain mixed with the primary field and do not reduce the transmitted flux. Components scattered through very small angles produce constant phase retardation in the transmitted field which can also be described by refraction (Sato 1982a, b). Components scattered through slightly larger angles produce lateral variations in the phase and amplitude of the primary field and reduce its lateral coherence.

Chernov (1960) derived expressions for the variance of the fluctuations of the phase, $\Delta\varphi$, and the natural logarithm of the amplitude, $\Delta \ln A$, of a wavefield that has propagated a distance l through a heterogeneous medium. Assuming an isotropic, Gaussian perturbation distribution, with variance H^2 and correlation length $a > \lambda$, he obtains

$$\langle|\Delta\varphi|^2\rangle = \frac{\Pi^{1/2}}{2} H^2 k^2 a L\left(1 + \frac{1}{D}\tan^{-1} D\right) \tag{9a}$$

$$\langle|\Delta \ln A|^2\rangle = \frac{\Pi^{1/2}}{2} H^2 k^2 a L\left(1 - \frac{1}{D}\tan^{-1} D\right), \tag{9b}$$

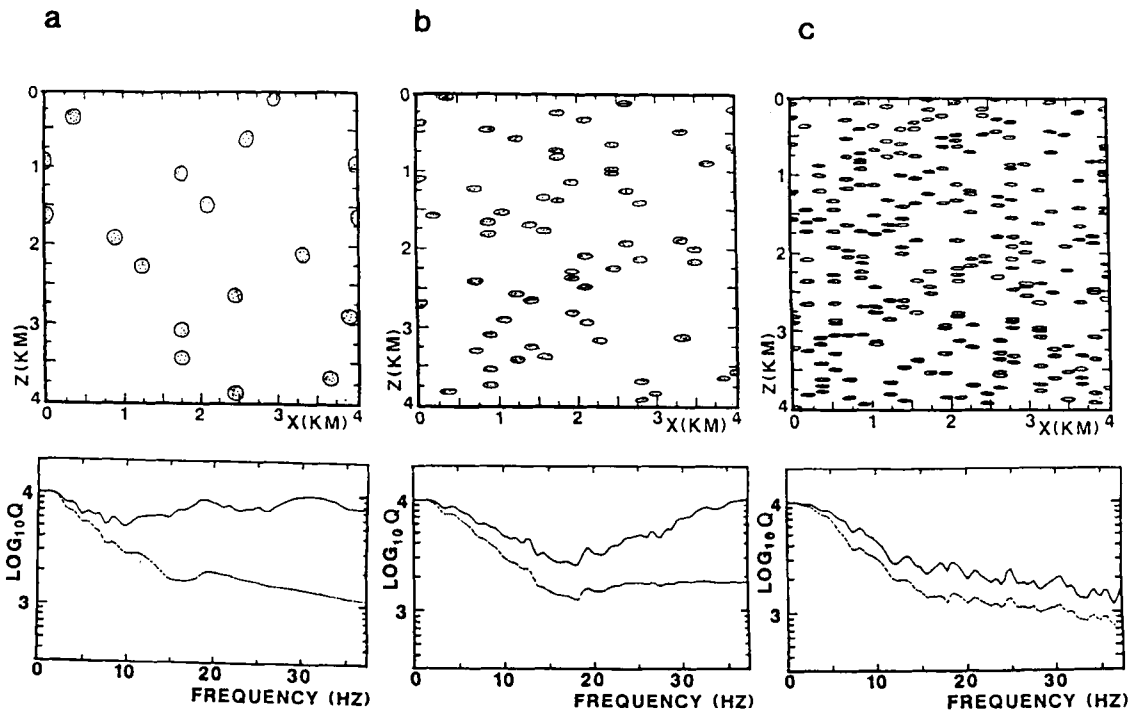

Figure 8. The variation with frequency of the attenuation due to scattering for three heterogeneous structures with differing values of c, the vertical correlation length. These structures are defined by a matrix of constant impedance with randomly distributed inclusions for which the impedance is 10 per cent higher. The anelastic Q is given a high value of 10 000 to demonstrate the scattering effects clearly. Bold lines show the attenuation due to components scattered through angles $\geq 90°$: dashed lines include all components scattered through angles $\geq 10°$.

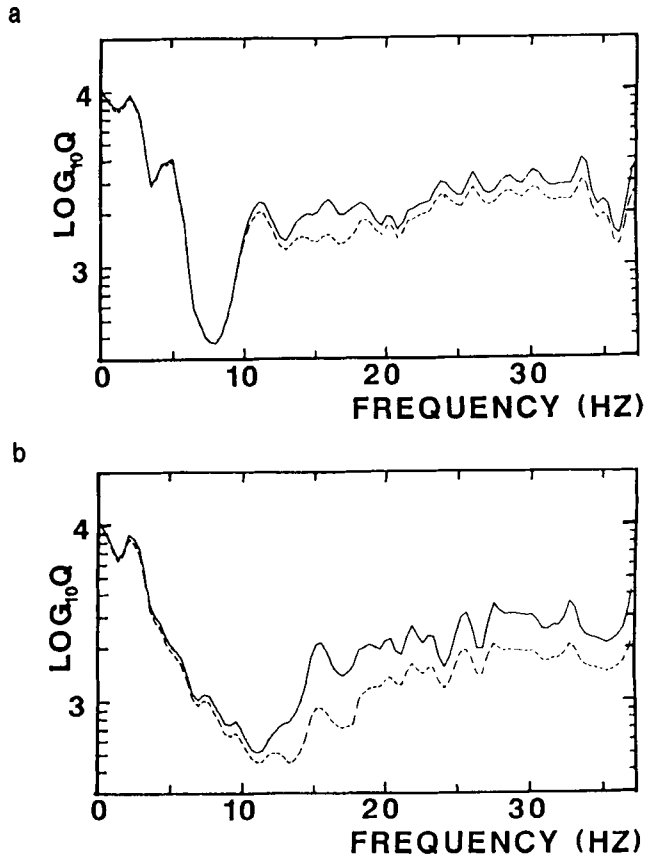

Figure 9. The variation with frequency of the attenuation due to scattering for the structures shown in Fig. 4(a and b). Bold lines indicate the loss due to components scattered through angles ≥90°: dashed lines include components scattered through angles ≥10°.

in which r_F is the Fresnel zone radius and D, the wave parameter, is defined by $D = 4L/ka^2$ and is proportional to the ratio of the area of the first Fresnel zone to that of the inhomogeneities. Due to the large area of the Fresnel zones for the lower crust D is much greater than 1 for all but the largest perturbations and (9) can be approximated to give the following simpler expressions

$$\langle|\Delta\varphi|^2\rangle \simeq (1 + a^2/r_F^2)\Pi^{1/2}H^2k^2aL \qquad (10a)$$

and

$$\langle|\Delta \ln A|^2\rangle \simeq (1 - a^2/r_F^2)\Pi^{1/2}H^2k^2aL. \qquad (10b)$$

Chernov also shows that the correlation length of the wavefield fluctuations produced by the components scattered by a heterogeneous structure is of the order of a, the horizontal length scale of the heterogeneities (Fig. 10).

These results can be extended to a medium described by an anisotropic Gaussian distribution of perturbations as defined in (5). For $ka \gg 1$ the isotropic and anisotropic distributions produce the same angular distribution of small-angle scattered components implying that they cause similar wavefield fluctuations.

Comparing the fields scattered by the isotropic and non-isotropic distributions indicates the following expressions for the variances of the wavefield phase and amplitude after propagation for a distance L through a medium characterized by an anisotropic, Gaussian distribution of perturbations

$$\langle|\Delta\varphi|^2\rangle \simeq (1 + a^2/r_F^2)\Pi^{1/2}H^2k^2cL \qquad (11a)$$

and

$$\langle|\Delta \ln A|^2\rangle \simeq (1 - a^2/r_F^2)\Pi^{1/2}H^2k^2cL. \qquad (11b)$$

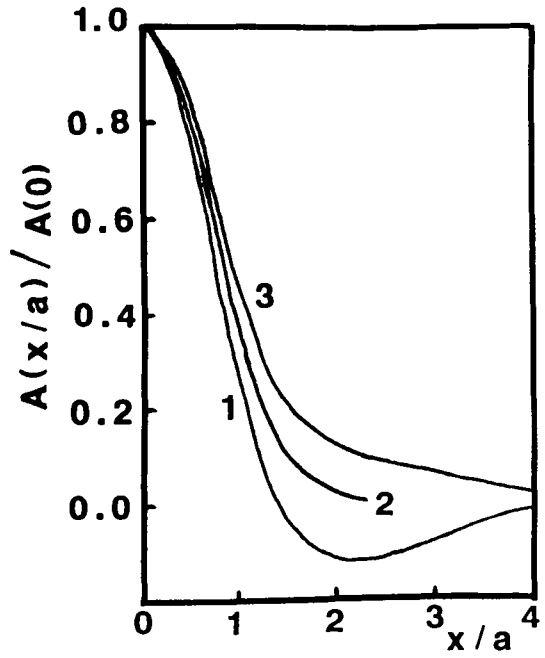

Figure 10. The normalized autocorrelation functions for (1) amplitude and (3) phase fluctuations along the wavefront for large D (after Chernov 1960). (2) shows a Gaussian variation of width a for comparison.

The observation of coherent reflections from the lower crust constrains the average degree of crustal heterogeneity. For a plane reflector in a heterogeneous medium the observed reflection will have fluctuations of phase and amplitude given by these equations with L equal to the total path length in the heterogeneous medium. The observation of coherent reflections from the lower crust implies that two-way travel through the crust has not generated sufficient small-angle scattered components to produce large fluctuations of phase and amplitude.

If $\langle|\Delta\varphi|^2\rangle$ and $\langle|\Delta \ln A|^2\rangle$ are both less than 1 for a path length L and $a \ll r_F$, (11a) and (11b) give the following condition:

$$H^2 < 1/(\Pi^{1/2}k^2cL), \qquad (12)$$

Fig. 11 shows the variation with c of the limits placed on H, the fractional standard deviation of the crustal elasticity, by the visibility of coherent reflections transmitted through various thicknesses of heterogeneous material. For example, assuming a seismic wavelength of 440 m and a crust characterised by $c = \lambda/4$, a coherent reflection from a depth of 25 km ($L = 50$ km) indicates that the average crustal H is less than 2.4 per cent.

This constraint complements the limits on the crustal heterogeneity calculated for crustal attenuation because the attenuation caused by large-angle scattering peaks for $c < \lambda/4$ and the incoherence caused by small-angle scattering is greatest for $c > \lambda/4$. There is an upper limit on the c

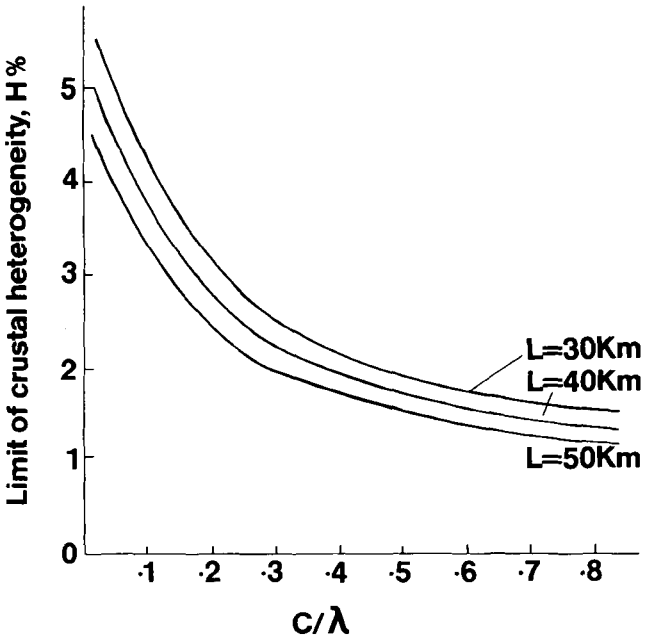

Figure 11. Plots showing the variation with c of the limits of H, the fractional standard deviation of the crustal elasticity, that are compatible with the observation of coherent reflections through thickness of heterogeneous crust of 15, 20 and 25 km respectively. These plots assume the seismic field is centred on 16 Hz.

values to which (12) applies because large heterogeneities which individually alter the phase of the wavefield by an amount comparable to Π can, in theory, be individually resolved and the seismic field can be corrected for their presence.

To visualize the effect of wavefield fluctuations on the resolution of the seismic experiment, a program has been written to calculate and display wavefields with variations of phase and amplitude given by (11). For simplicity, the wavefield autocorrelation functions in (11) are approximated by Gaussian variations with correlation length a, i.e.

$$M_{\varphi}(x) \simeq (1 + a^2/r_F^2)\Pi^{1/2}H^2k^2cL \exp(-x^2/a^2) \tag{13a}$$

and

$$M_{\ln A}(x) \simeq (1 - a^2/r_F^2)\Pi^{1/2}H^2k^2cL \exp(-x^2/a^2). \tag{13b}$$

Particular phase and amplitude functions, $\varphi(x)$ and $A(x)$, are calculated exhibiting these autocorrelation functions and the wavefield displacement, $v(x, t)$, is formed using the following relationship

$$v(x, t) = A(x) \cdot u[t - t_0 - \varphi(x)/\omega_0], \tag{14}$$

in which $u(t)$ is the source function, ω_0 is the peak frequency of the wavefield and t_0 is the travel time, L/α.

This is not a complete model of the physics described by Chernov as, apart from the approximation of the autocorrelation functions, it also neglects the cross-correlations between $\Delta\varphi$ and $\Delta \ln A$. It does, however, help estimation of the depth at which the primary wavefield becomes disrupted to the extent that resolution of the most prominent geological features becomes impossible.

Fig. 12 shows the development of incoherence in a wavefield centred on 16 Hz propagating through a structure with 5 per cent standard deviation and correlation lengths of

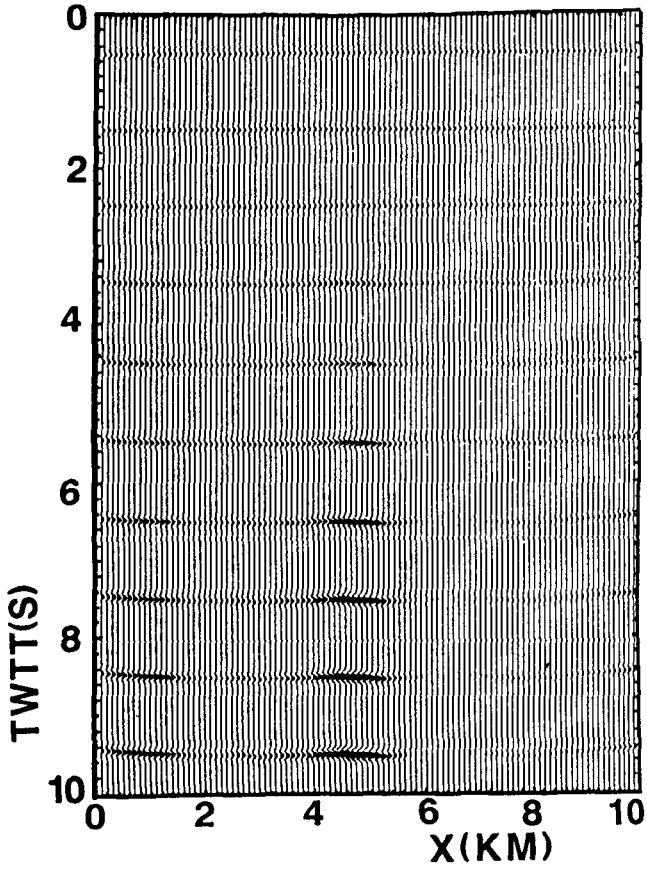

Figure 12. The development of fluctuations in a plane reflection centred on 16 Hz after it has propagated two ways through a heterogeneous structure characterized by 5 per cent standard deviation and correlation lengths $a = 1000$ m and $c = 50$ m.

1000 m horizontally and 50 m vertically. The wavefronts represent two-way travel through a heterogeneous crust and planar reflection. Fig. 12 shows that these crustal variations would make it difficult to recognize a plane reflector at a depth greater than 16 km. The development of incoherence due to small angle scattering is independent of both the amplitude of the field incident on the reflector and its reflectivity.

Figure 13 represents wavefronts after propagation through a structure characterized by 5 per cent standard deviation with horizontal and vertical correlation lengths of 100 and 50 m respectively. Fig. 13(a–c) is calculated for wavefields centred on 10, 16 and 25 Hz respectively and show the rapid increase in the degree of incoherence for components of increasing frequency. Fig. 14 wavefronts after propagation through a structure characterized by 5 per cent standard deviation with horizontal and vertical correlation lengths of 200 and 100 m respectively. Comparison of Figs 13b and 14 shows the increased degree of incoherence caused by larger scale perturbations.

Fig. 15 shows a sample of a deep reflection profile with a very high degree of reflectivity but lacking identifiable coherent reflections. This very common type of lower-crustal reflectivity could be caused by the effects described in this section. Although scattering theory based on (3) provides useful results relating properties of the seismic field to the statistical properties of the crust it cannot be readily

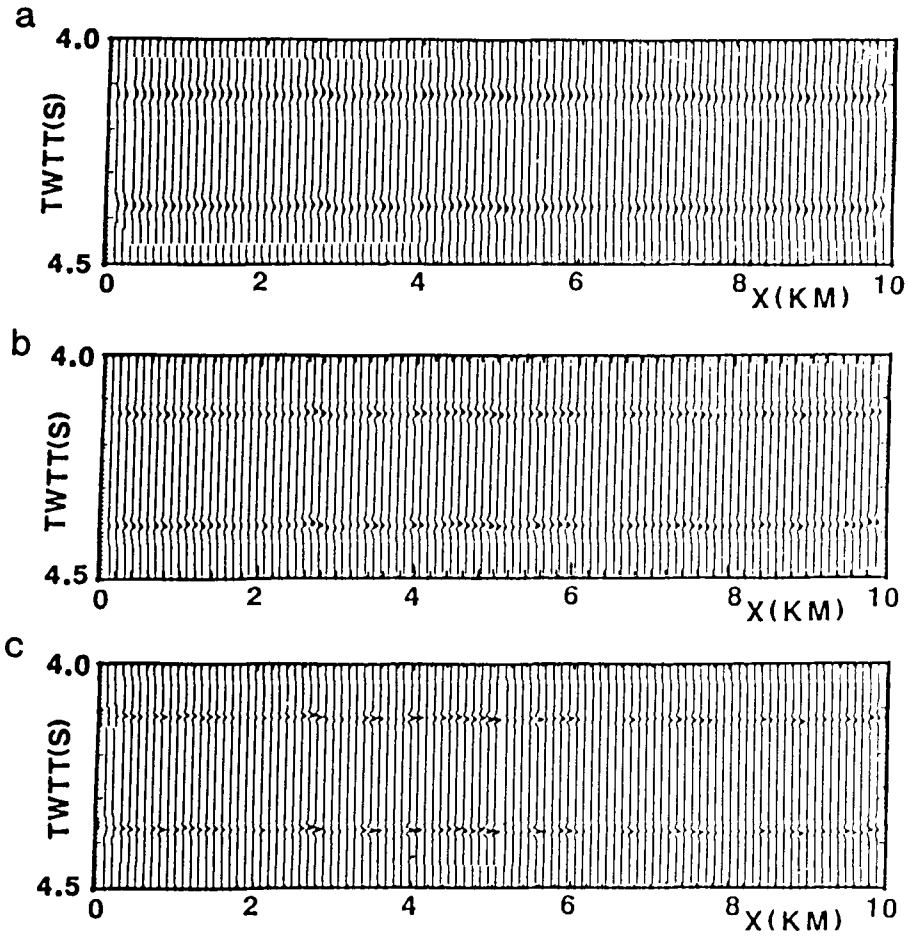

Figure 13. The plane reflections shown are centred on 10, 16 and 25 Hz respectively and have propagated two ways through a heterogeneous medium characterized by 5 per cent standard deviation and correlation lengths $a = 100$ m and $c = 50$ m. The incoherence caused by scattering increases rapidly with increasing frequency.

applied to the interpretation of real seismic data because it cannot handle the possibility of unknown spatial variations of the statistical crustal properties. The block of data shown may contain components which have sampled volumes of crust characterized by very different distributions of elastic variations.

THE VALIDITY OF FIRST-ORDER SCATTERING THEORY

According to Chernov (1960), first-order scattering theory is applicable when a small proportion of the primary flux is scattered. This is because the theory assumes that the primary field is unchanged by the variations of the medium and because the effects of multiple-scattering are neglected. A small proportion of primary-scattering ensures an insignificant degree of multiple-scattering.

Hudson & Heritage (1981) subsequently derived a new condition for the validity of the first-order approximation by considering it as the first term of an infinite series the subsequent terms of which represent multiply-scattered components. The new condition ensures the accuracy of the solution *at all points and times* and is far more difficult to satisfy than Chernov's condition which refers to statistical

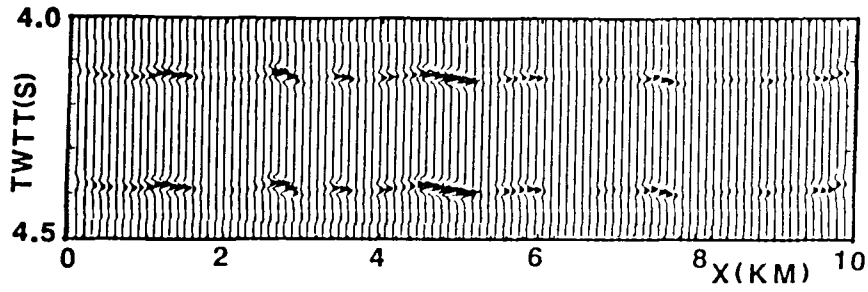

Figure 14. The wavefield shown is centred on 16 Hz and has propagated two ways through a heterogeneous medium characterized by 5 per cent standard deviation and correlation lengths $a = 200$ m and $c = 100$ m.

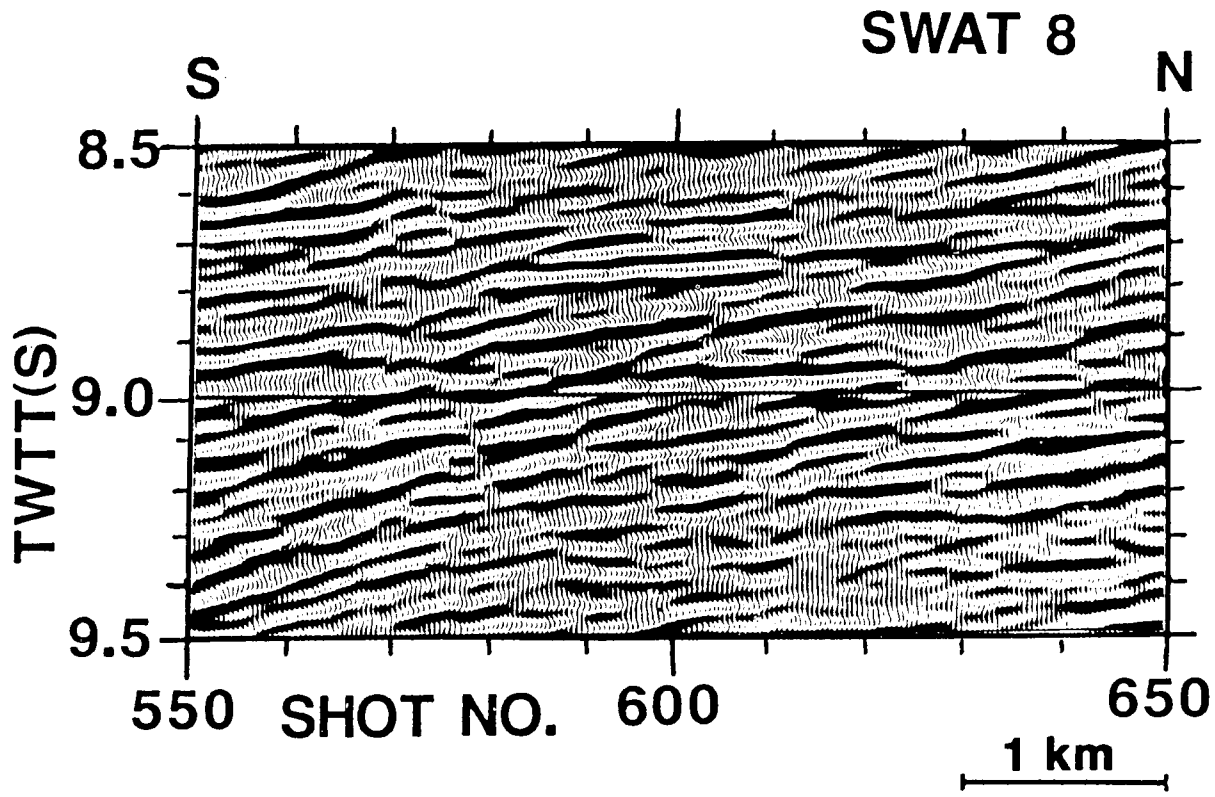

Figure 15. A typical sample of highly reflective lower crust which lacks clearly defined individual reflectors taken from the Southern end of the SWAT 8 profile collected by BIRPS (BIRPS & ECORS 1986).

field properties only (i.e. Chernov's condition allows solutions which may be locally inaccurate if the scattered components are in some respect organized).

Chernov's limit is more suitable for the work presented here because we are concerned with statistical averages of the scattered field rather than specific solutions. Also, there is no *a priori* reason to expect any strong organisation of the components of the wavefield scattered by variations of the lower crust.

Applying Chernov's validity test to a reflection from a depth of 12.5 km (i.e. a path length of 25 km) in a crust characterized by $H = 5$ per cent the fraction of incident flux scattered is less than 20 per cent, i.e. mid-crustal reflections are close to the limit of validity of first-order scattering. For a reflection from a depth of 25 km (path length 50 km) in a similar crust the scattered fraction rises to almost 40 per cent implying that multiple scattering must be taken into account for reflections from the lower crust.

However, first-order scattering can be applied to the calculation of the attenuation due to scattering because Q is calculated by summing the components scattered by a small crustal volume. Using first-order scattering to estimate the wavefield incoherence gives a conservative estimate of the effect of all scattering processes because the multiply-scattered components cause further loss of coherence.

CONCLUSIONS

The effect on the seismic wavefield of mild variations of crustal elasticity can be modelled using first-order scattering theory. This model shows that statistically defined distributions of crustal variations that are too small to be resolved individually can affect the reflections observed in a deep seismic reflection profile.

Crustal heterogeneities on length scales smaller than the seismic wavelength cause components of the seismic wavefield to be scattered through large angles. These components are removed from the transmitted wavefield causing frequency-dependent attenuation that is comparable with the low degree of attenuation measured for the crust for fractional variations of the elasticity of a few percent. Large scale variations of the crustal elasticity produce wavefield components scattered through small angles. These reduce the coherence of the seismic field causing fluctuations of phase and amplitude on a length-scale comparable with the horizontal length-scale of the crustal variations.

The observation of coherent seismic reflections from the lower crust and the high Q value exhibited by the crust both constrain the fractional variations of the crustal elasticity measured on a wide range of vertical length scales to a few percent. This very low degree of heterogeneity represents an average over the whole of the crust. Our knowledge of the physical properties of the shallower parts of the crust can be used to further constrain the properties of the lower crust.

The constraints placed on crustal heterogeneity by scattering theory do not exclude the large variations of crustal elasticity indicated by the reflectivity of the lower crust. The limits on the range of elasticity derived in this paper represent a statistical average over the whole crust. Individual contacts with large elastic contrasts do not significantly alter the statistics of the whole crust. However, scattering theory does limit the degree to which the crust

can consist of laminated structures with alternating layers of higher and lower acoustic impedance on the scale of the seismic wavelength because the high reflectivity of these structures would be accompanied by a very rapid attenuation of the seismic field.

ACKNOWLEDGMENTS

This work was done while I was studying for a PhD. with the BIRPS group at the Bullard Laboratory, University of Cambridge. I was funded during this period by a Shell Studentship. I thank my colleagues at BIRPS and especially my supervisor, Drum Matthews, for all their assistance. I gratefully acknowledge the assistance of Carrington Computer Consultants and the Civil Aviation Authority in the preparation of this paper. Cambridge University Department of Earth Sciences contribution number ES 1252.

REFERENCES

Aki, K., 1973. Scattering of P waves under the Montana LASA, *J. geophys. Res.*, **78,** 1334–1346.

Aki, K., 1981. Source and scattering effects on the spectra of small local earthquakes, *Bull. seism. Soc. Am.*, **71,** 1687–1700.

Aki, K. & Bhouet, B., 1975. Origin of coda waves, source attenuation and scattering effects, *J. geophys. Res.*, **80,** 3322–3342.

Aki, K. & Richards, P. G., 1980. *Quantitative Seismology: Theory and Methods*, Vols. 1 & 2, W. H. Freeman, San Francisco.

BIRPS & ECORS (Cheadle, M., Matthews, D., McGeary, S., Warner, M., Armstrong, E. J., Blundell, D., Chadwick, A., Day, G., Edwards, J. W. F., Mascal, A., Gariel, O., Montadert, L., Lefort, J. P., Le Gall, B., Sibouet, J.-C., Cazes, M. & Schroeder, I. J.), 1986. Deep seismic reflection profiling between England, France and Ireland, *J. geol. Soc. Lon.*, **143,** 45–52.

Capon, J., 1974. Characterization of crust and upper mantle structure under LASA as a random medium, *Bull. seism. Soc. Am.*, **64,** 235–266.

Chernov, L. A., 1960. *Wave Propagation in a Random Medium*, McGraw-Hill, New York.

Clowes, R. M. & Kanasewich, E. R., 1972. Seismic attenuation and the nature of reflecting horizons within the crust, *J. geophys. Res.*, **75,** 6693–6705.

Haddon, R. A. W. & Cleary, J. R., 1974. Evidence for scattering of seismic PkP waves near the mantle-core boundary, *Phys. Earth planet. Int.*, **8,** 211–234.

Hagedoorn, J. G., 1954. A process of seismic reflection interpretation, *Geophys. Prospect.*, **2,** 85–127.

Hudson, J. A. & Heritage, J. R., 1981. The use of the Born approximation in seismic scattering problems, *Geophys. J. R. astr. Soc.*, **66,** 221–240.

Knopoff, L. & Hudson, J. A., 1964. Scattering of elastic waves by small inhomogeneities, *J. acoust. Soc. Am.*, **36,** 338–343.

Knopoff, L. & Hudson, J. A., 1967. Frequency dependence of scattered elastic waves, *J. acoust. Soc. Am.*, **42,** 18–20.

Meissner, R., 1973. The 'Moho' as a transition zone, *Geophys. Surv.*, **1,** 195–216.

Meissner, R., 1986. Twenty years of deep seismic reflection profiling in Germany—a contribution to our knowledge of the lower Variscan crust, in *The Nature of the Lower Crust*, ed. J. Hall, Geological Society of London.

Pekeris, C. L., 1947. Note on the scattering of radiation in an inhomogeneous medium, *Phys. Rev.*, **71,** 268–269.

Phinney, R. A. & Jurdy, D. M., 1979. Seismic imaging of the deep crust, Geophysics, **44,** 1637–1660.

Sato, H., 1982a. Amplitude attenuation of impulsive waves in random media based on travel time corrected mean wave formalism, *J. acoust. Soc. Am.*, **71,** 559–564.

Sato, H., 1982b. Attenuation of S waves in the lithosphere due to scattering by its random velocity structure, *J. geophys. Res.*, **87,** 7779–7785.

Wu, R.-S., 1982. Attenuation of short period seismic waves due to scattering, *Geophys. Res. Lett.*, **9,** 9–12.

Wu, R.-S., 1985. Multiple scattering and energy transfer of seismic waves—separation of scattering effect from intrinsic attenuation—I. Theoretical modelling, *Geophys. J. R. astr. Soc.*, **82,** 57–80.